

Non-magnetic Fractional Conductance in High Mobility InAs Quantum Point Contacts

I. Villar Rodriguez,^{1,2,*} Y. Gul,^{1,2} C.P. Dempsey,³ J.T. Dong,⁴ S.N. Holmes,² C.J. Palmstrøm,^{3,4} and M. Pepper^{1,2}

¹*London Centre for Nanotechnology, University College London,
17-19 Gordon Street, London WC1H 0AH, United Kingdom*

²*Department of Electronic and Electrical Engineering, University College London,
Torrington Place, London WC1E 7JE, United Kingdom*

³*Department of Electrical and Computer Engineering,
University of California, Santa Barbara, CA 93106, USA*

⁴*Materials Department, University of California, Santa Barbara, CA 93106, USA*

(Dated: March 12, 2025)

In this letter, we report the magneto-electronic properties of high mobility InAs quantum point contacts grown on InP substrates. The 1D conductance reaches a maximum value of 17 plateaus, quantized in units of $2e^2/h$, where e is the fundamental unit of charge and h is Planck's constant. The in-plane effective g-factor was estimated to be -10.9 ± 1.5 for subband $N = 1$ and -10.8 ± 1.6 for subband $N = 2$. Furthermore, a study of the non-magnetic fractional conductance states at $0.2(e^2/h)$ and $0.1(e^2/h)$ is provided. While their origin remains under discussion, evidence suggests that they arise from strong electron-electron interactions and momentum-conserving backscattering between electrons in two distinct channels within the 1D region. This phenomenon may also be interpreted as an entanglement between the two channel directions facilitated by momentum-conserving backscattering.

I. INTRODUCTION

Quantization of conductance in units of $2e^2/h$ in one-dimensional (1D) quantum point contacts (QPCs) was first observed by D.A. Wharam [1] and B.J. van Wees [2] when investigating a gate-controlled channel defined in the two-dimensional electron gas (2DEG) of a GaAs/AlGaAs heterostructure. Since then, many reports have studied the interesting physics of these constrictions: the effect of a source-drain bias voltage [3–5], the appearance of the 0.7 conductance anomaly [6–9] and other many-body effects [10–12]. One of the most highlighted recent advances in the field demonstrated the potential to spatially manipulate electron spins in a QPC [13, 14]. This is a crucial component for spin-based technologies. Additionally, the realization of an all-electrical spin field-effect transistor was achieved through the implementation of two QPCs [15].

1D quantization of conductance is observed in ballistic constrictions where the mean free path of the electrons is larger than the size of the split gates. Therefore, high quality heterostructures with high 2DEG electron mobility are required. Furthermore, a 2DEG with strong spin-orbit coupling (SOC) would facilitate the manipulation of the electron spins. A material that meets all these requirements would be an ideal candidate for spintronic and quantum information devices.

High electron mobility InAs quantum wells (QWs) have been grown in both lattice-matched GaSb [16, 17] and lattice-mismatched InP [18, 19] substrates. However, the reported presence of side wall conduction in

InAs QWs grown on GaSb substrates [20] makes InP a better choice. Moreover, recent advancements [21] in wafer manufacturing have improved upon the current state-of-the-art QW thickness t_{QW} ($t_{QW} = 4$ nm for $\text{In}_{0.75}\text{Al}_{0.25}\text{As}$ [19] barrier layers and $t_{QW} = 7$ nm for $\text{In}_{0.81}\text{Al}_{0.19}\text{As}$ [22] barrier layers) of InAs QWs grown on InP substrates. This advancement shows an improvement in the highest achievable mobility. Other significant properties of InAs include its small effective mass [23] and its large bulk g-factor. For comparison, the g-factor of bulk InAs is -15 [24], which is considerably larger than that of InGaAs (-9) [25] or GaAs (-0.44) [26]. Furthermore, InAs exhibits strong SOC that allows efficient control of spin currents. The large g-factor of InAs leads to Zeeman splitting at low magnetic fields, which in proximity to an s-wave superconductor could introduce Majorana zero modes [27–30] that can be utilized for topological quantum computing applications [31]. Several studies have already been conducted on 1D InAs QPCs [18, 32–34], with a maximum of eight pronounced quantized conductance plateaus observed at 1.5 K [35].

Strong electron-electron interactions occur when the carrier density in the QPC is low. In this state, non-magnetic fractional quantization of conductance has previously been reported in strained-Ge [36], InGaAs [37] and GaAs [38] QWs. Although the origin of these new quantum states is not fully understood, their study could lead to future applications in quantum computing.

In this work, we present the magneto-transport properties of gate-defined 1D QPCs fabricated on InAs QWs grown on InP substrates, with QW thicknesses exceeding those reported in earlier studies. We demonstrate clean and controllable 1D behavior. Furthermore, strong electron-electron interactions at low carrier densities are investigated. Here, non-magnetic fractional quantization

* uceevi@ucl.ac.uk

of conductance is observed, and possible effects leading to this phenomenon are discussed.

II. DEVICE FABRICATION AND EXPERIMENTAL SETUP

The device presented in this work is an InAs QW heterostructure grown on a semi-insulating Fe-doped InP (001) substrate by molecular beam epitaxy (MBE). The 2DEG lies 130 nm below the surface and is surrounded by $\text{In}_{0.72}\text{Ga}_{0.28}\text{As}$ cladding layers. The width of the QW is 16 nm, exceeding the maximum previously achievable width for InAs QWs grown on InP substrates [19, 22]. A more detailed explanation of the growth conditions can be found in Ref. [21].

For 1D electrical and magneto-transport measurements, Hall bars of $1400\ \mu\text{m}$ in length and $80\ \mu\text{m}$ in width were fabricated. Using a mixture of $\text{H}_2\text{SO}_4:\text{H}_2\text{O}_2:\text{H}_2\text{O}$ (1:8:120), the Hall bar mesa was etched so that the QPC channel lies along the $[1\bar{1}0]$ direction. AuGeNi Ohmic contacts connecting the 2DEG and the surface were evaporated onto the sample and annealed at $450\ \text{°C}$ for 2 minutes. To insulate the 2DEG from the gates, a 35 nm Al_2O_3 dielectric layer was deposited using atomic layer deposition (ALD). Windows for the Ohmic contacts were opened by etching through the dielectric. Finally, the split gates and top gates were patterned onto the wafer using electron beam lithography (EBL). Cross-linked polymethyl methacrylate (PMMA) was used as a dielectric between the split gates and the top gates, and Ti/Au was deposited to form the gates. The results presented in this letter were obtained from split gates measuring 500 nm in length and width or 400 nm in length and 500 nm in width. At 1.5 K, the 2DEG carrier density is $3.6 \times 10^{11}\ \text{cm}^{-2}$, and the electron mobility is $9.3 \times 10^5\ \text{cm}^2/\text{Vs}$. The effective electron mass and the Rashba coefficient were determined as $(0.031 \pm 0.002)m_e$, where m_e is the rest electron mass, and $12 \times 10^{-12}\ \text{eV}\cdot\text{m}$, respectively [21].

In all experiments, the two-terminal differential conductance (G) was measured as a function of split gate voltage (V_{sg}) at a constant top gate voltage (V_{tg}), while a $10\ \mu\text{V}$ AC voltage at 33 Hz was applied. The measurements were taken in a cryo-free dilution refrigerator at 220 mK over multiple cooldowns. The measurement configuration is shown in Fig. 1.

III. RESULTS AND DISCUSSION

A. 1D conductance quantization

Fig. 2 illustrates the quantized 1D conductance as the split gate voltage is raised from the pinch-off state. We observe seventeen plateaus quantized in units of $2e^2/h$, which is twice the number reported in earlier studies

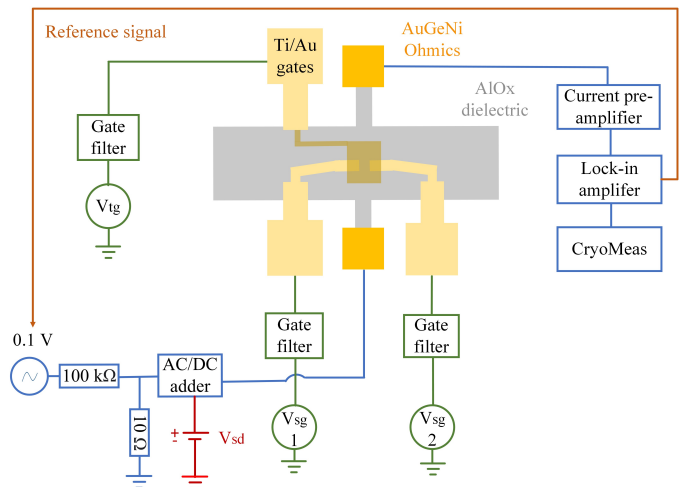


FIG. 1. Two-terminal conductance measurement setup. A constant AC differential voltage drop across the device is applied using a potential divider. A DC source-drain bias voltage, V_{sd} , can be superimposed onto the signal using a AC/DC adder. All gates are protected by a low pass gate filter. The outgoing signal is amplified by a current pre-amplifier and measured by a lock-in amplifier. CryoMeas [39] is the program utilized to record the data.

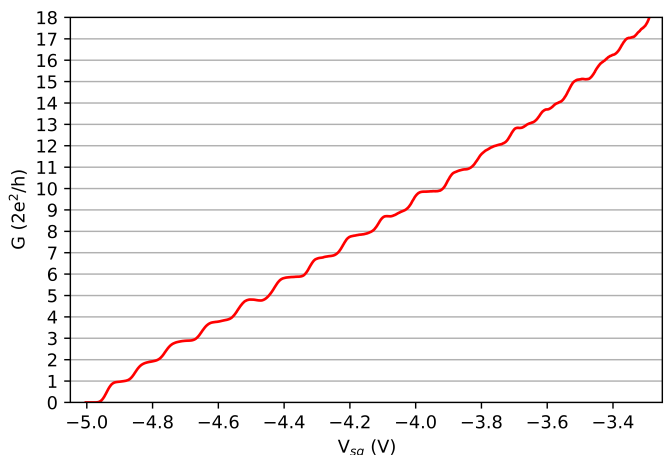


FIG. 2. G as a function of V_{sg} when $V_{tg} = 0\ \text{V}$. The split gate dimensions are 400 nm in length and 500 nm in width, and up to seventeen plateaus quantized in units of $2e^2/h$ can be observed. The series resistance for this measurement was $1.3\ \text{k}\Omega$, determined individually for each cooldown and each QPC.

[18, 32–35]. This finding underscores the high material quality and indicates ballistic transport in the gate-defined 1D QPCs. The observed conductance trace is consistent across different cooldown cycles, but it shows a gradual shift toward more negative pinch-off voltages with repeated voltage sweeps. This drift can be attributed to interactions between large applied split gate voltages and charge traps within the dielectric layer [35]. To mitigate this, we employed slightly larger split gates

(500 nm in width and length), resulting in a more stable pinch-off voltage and minimal drift - suggesting dielectric charging as a primary cause of the shift.

B. Calculation of the in-plane effective g-factor

The effective g-factor, g^* , was estimated by analyzing the Zeeman splitting under an applied in-plane magnetic field, B , and the subband spacing by applying a DC source-drain bias voltage, V_{sd} , using the expression [40]

$$|g^*| = \frac{1}{\mu_B} \frac{d(\Delta E_z)}{dB} = \frac{e}{\mu_B} \frac{\delta V_{sd}}{\delta V_{sg}} \frac{\delta V_{sg}}{\delta B}, \quad (1)$$

where μ_B is the Bohr magneton and E_z represents the Zeeman energy.

Clear Zeeman spin-splitting is observed when applying an in-plane magnetic field, as shown in Fig. 3. The splitting is visible at approximately 2 T. As the magnetic field increases, odd-numbered plateaus emerge while the even-numbered disappear. At sufficiently high magnetic fields, crossing of the spin-split subbands is observed before the reappearance of the even-numbered plateaus. By extracting the crossover point of the spin-split subbands, $\delta V_{sg}/\delta B$ can be determined.

Fig. 4(a) depicts 1D conductance traces under varying DC bias voltages. When a high DC bias is applied, the momentum degeneracy is lifted [5] and the spin-degenerate plateaus evolve into $0.5(2e^2/h)$, $1.5(2e^2/h)$, $2.5(2e^2/h)$, etc. For negative DC bias, this behavior is apparent, however, for positive DC bias, a distinct plateau at $0.25(2e^2/h)$ can be seen. This effect has been observed before in InGaAs [40] and GaAs [5] heterostructures, where the asymmetric behavior was attributed to

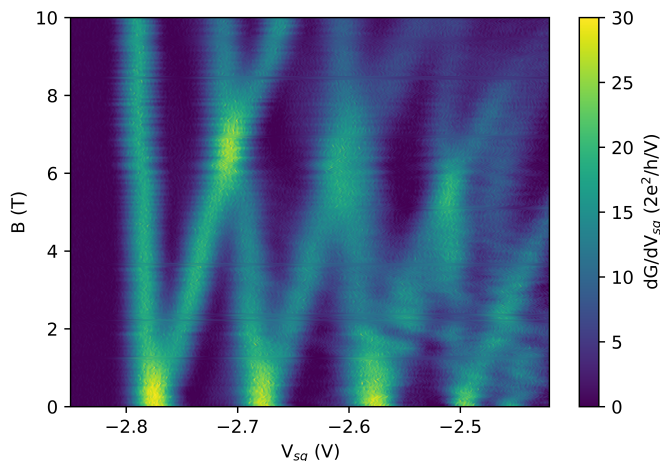


FIG. 3. Transconductance (dG/dV_{sg}) plotted as a function of in-plane B on the y-axis and V_{sg} on the x-axis. The bright yellow lines correspond to rises in conductance, while the blue dark regions signify the quantized plateaus. Subband crossings are also visible.

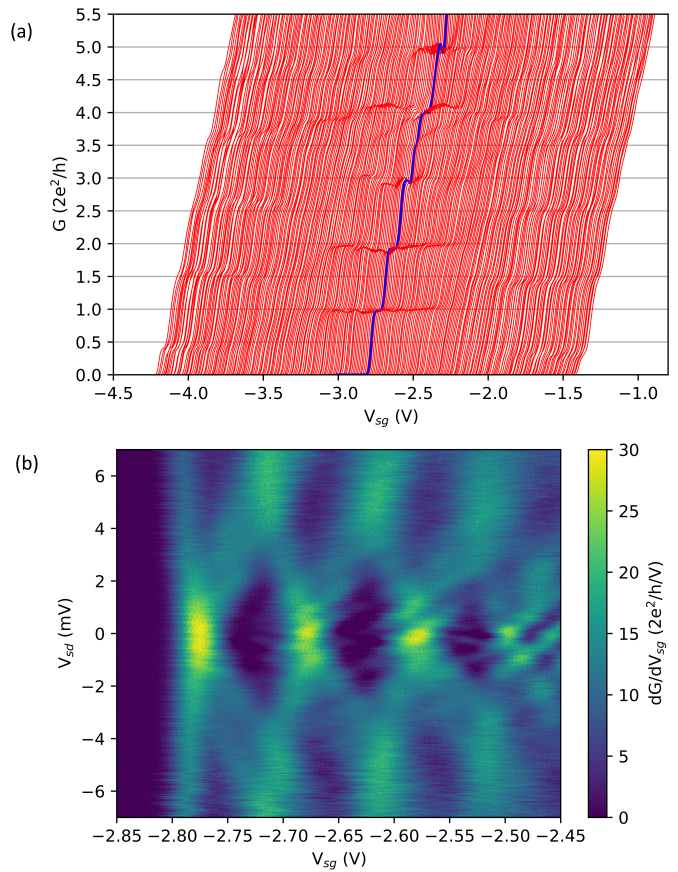


FIG. 4. (a) G as a function of V_{sg} for different values of V_{sd} varying from -7 mV (left) to 7 mV (right) in 0.05 mV steps. The blue trace corresponds to $V_{sd} = 0$ V. For display purposes, the traces have been shifted laterally by 10 mV. The series resistance for this measurement was 1.6 k Ω . (b) Transconductance (dG/dV_{sg}) plotted as a function of V_{sd} on the y-axis and V_{sg} on the x-axis. The blue dark regions correspond to the quantized plateaus, while the brighter yellow regions indicate the subband transitions where dG/dV_{sg} is large.

the formation of a density wave or Skyrmion [40]. In the case of GaAs [5], the emergence of the $0.25(2e^2/h)$ structure was linked to the creation of a unidirectional spin-polarized current. The transconductance as a function of V_{sd} and V_{sg} in Fig. 4(b) shows how the even diamonds evolve into odd-quantized values. The intersection where two subbands cross can be used to extract $\delta V_{sd}/\delta V_{sg}$. The effective g-factor of the material was then determined using Eq. 1. The variables necessary for this calculation are provided in Table I. The computed effective g-factor is of similar order to that reported in previous studies on InAs QWs [35].

TABLE I. Extracted parameters for the Zeeman splitting and subband spacing crossings used to determine g^* .

Subband	$N = 1$	$N = 2$
$\delta V_{sg}/\delta B (10^{-2} \text{ V/T})$	1.21 ± 0.06	1.43 ± 0.11
$\delta V_{sd}/\delta V_{sg} \text{ (mV/V)}$	52.2 ± 6.6	43.8 ± 5.5
g^*	-10.9 ± 1.5	-10.8 ± 1.6

C. Non-magnetic fractional conductance quantization

The observation of non-magnetic fractional quantization of conductance typically occurs at low carrier densities and asymmetric confining potentials [36–38]. To investigate fractional conductance quantization in the 1D InAs QPCs, the carrier density was reduced by applying a negative voltage to the top gate. As the top gate voltage became increasingly negative, a sudden transition in conductance was observed in the ground state, shifting from $2e^2/h$ to $2(2e^2/h)$. This transition preceded the emergence of fractional conductance plateaus and may suggest the formation of a zigzag incipient Wigner crystal [12].

The 0.1 and 0.2 (e^2/h) fractions, previously observed in InGaAs [37], are seen in InAs at low carrier densities. Both fractional states persist even as the temperature increases, as shown in Fig. 5. Combined with multiple cooldown measurements, this suggests that these non-magnetic fractional states are not caused by disorder. The slight lifting of the plateaus from their quantized value with temperature is consistent with predictions by G. Shavit and Y. Oreg [41]. Their theoretical model allows for non-magnetic fractional conductance quantization through momentum-conserving backscattering of electrons in two distinct spin subbands or transverse channels, such as those formed in a zigzag incipient Wigner crystal. The resulting conductance is given by

$$G = \frac{(n_1 - n_2)^2}{n_1^2 + n_2^2} \left(\frac{e^2}{h} \right), \quad (2)$$

where n_i represents the number of backscattered electrons from subband i . This model predicts the 0.2 (e^2/h) plateau when $n_1 = 1, 2$ and $n_2 = 2, 4$, but it does not explain the formation of the 0.1 (e^2/h) plateau. A scenario where channel 1 is decoupled from the leads but confined within the wire and strongly interacts with the other channel could yield a conductance of $G = n_1^2/(n_1^2 + n_2^2)$ [41], potentially explaining the 0.1 (e^2/h) state for $n_1 = 1$ and $n_2 = 3$. However, no evidence of channel 1 being confined within the wire is observed in this study. Further investigations are necessary to elucidate the origin of the 0.1 (e^2/h) plateau.

Applying a magnetic field to these fractional states reveals deviations from previous observations in InGaAs systems [37]. In InGaAs, the fractions persisted under the application of an in-plane magnetic field parallel to

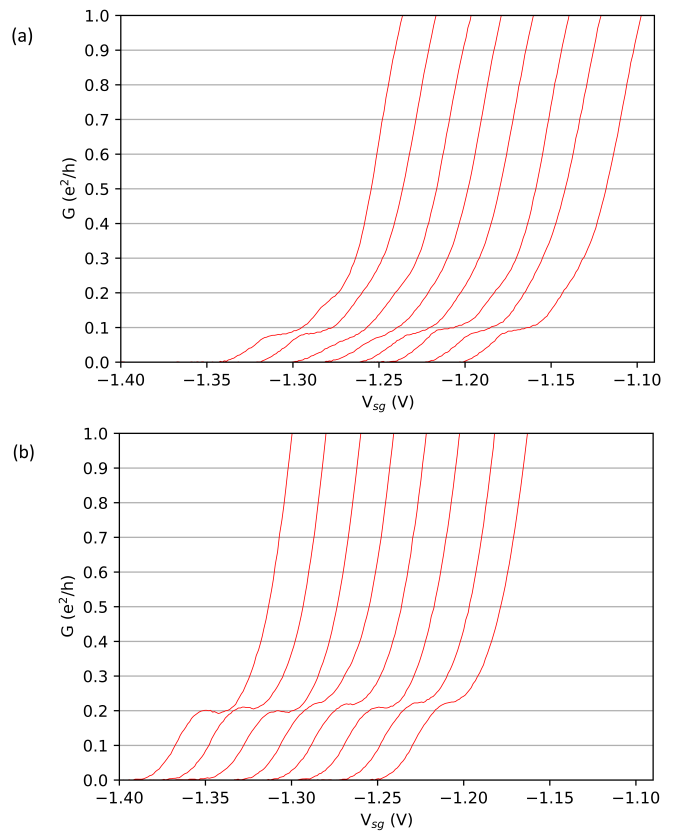


FIG. 5. Temperature dependence of the (a) 0.1(e^2/h) and (b) 0.2(e^2/h) plateaus. The 0.1(e^2/h) plateau was observed at $V_{tg} = -3.03$ V, while the 0.2(e^2/h) plateau was observed at $V_{tg} = -2.93$ V. The temperature was varied from 220 mK (left) up to 920 mK (right) in 100 mK steps. For clarity, the traces have been shifted horizontally by 20 mV.

the current direction but disappeared when the field was applied in-plane and perpendicular to the current. In contrast, in InAs, the fractions vanish under an in-plane magnetic field regardless of its orientation relative to the current.

In InGaAs, this behavior was attributed to Rashba spin splitting. When the magnetic field was parallel to the current, a spin gap formed, enabling backscattering between the spin-split subbands. Conversely, when the magnetic field was perpendicular, one of the spin-split subbands shifted up in energy, preventing backscattering and thereby causing the fractions to disappear. However, the distinct behavior observed in our InAs devices suggests that these states are not spin polarized and do not arise from momentum-conserving backscattering between electrons in different spin subbands.

This difference can be explained by examining the wafer structures. The InGaAs wafers are Si-doped, which enhances Rashba asymmetry across the QW, while the InAs wafers are undoped. This doping alters the shape of the confining potential and, consequently, the Rashba splitting, leading to the observed variations in behavior.

If a zigzag incipient Wigner crystal has formed, momentum-conserving backscattering of electrons can occur between the two transverse channels of the zigzag. Consequently, the two zigzag channels could become entangled [41].

Fig. 6 shows the conductance under varying lateral asymmetric potentials, ΔV_{sg} , with fraction formation preserved in one bias direction but suppressed in the opposite. This suggests that one direction of lateral asymmetry may enhance electron-electron interactions, promoting zigzag formation, while the opposite direction weakens these interactions, returning the electrons to their 1D arrangement. Further experiments, such as transverse electron focusing, are needed to conclusively identify zigzag formation.

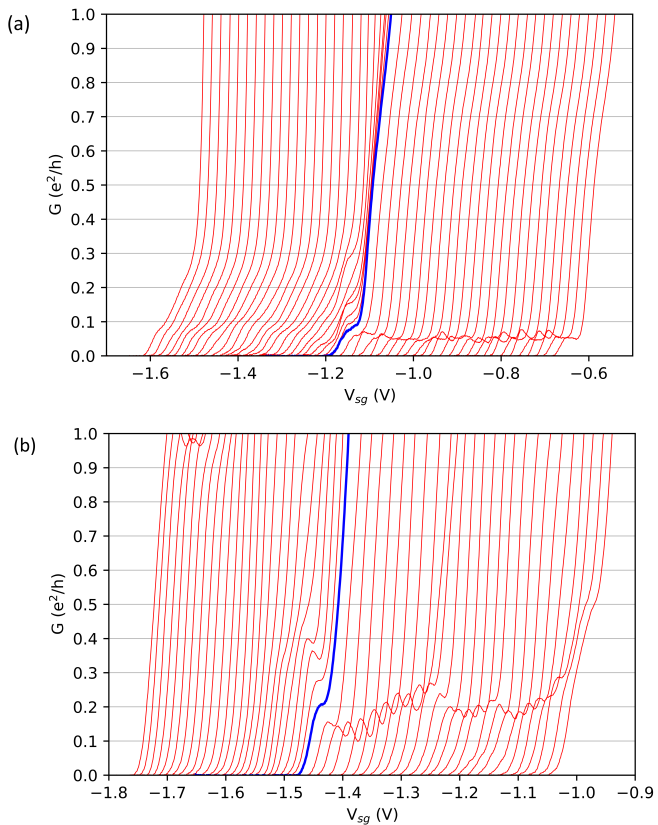


FIG. 6. G as a function of V_{sg} with varying degrees of lateral asymmetric confinement, reaching a maximum shift of $\Delta V_{sg} = \pm 0.5$ V on each side of the graph, for the (a) $0.1(e^2/h)$ and (b) $0.2(e^2/h)$ plateaus. The blue trace corresponds to symmetrically biased split gates. For the $0.1(e^2/h)$ plateau, its value decreases in the direction of the preserved bias, while for the $0.2(e^2/h)$ plateau, it oscillates around its nominal value.

An interesting aspect of these fractional electron states is their potential to demonstrate fractional charge. Numerous studies [42–46] have investigated fractional

charge in fractional quantum Hall effect (FQHE) systems through shot noise experiments. The detection of fractional charge in these InAs fractional conductance states could provide new opportunities to investigate whether they exhibit non-Abelian properties, potentially playing a crucial role in the development of topological quantum computing.

IV. CONCLUSION

In summary, we have demonstrated high mobility ballistic transport in 1D InAs QPCs, with conductance quantization observed up to $17(2e^2/h)$. The in-plane effective g-factor was calculated to be -10.9 ± 1.5 for $N = 1$ and -10.8 ± 1.6 for $N = 2$, determined from the intersection of spin-split and momentum-split subbands.

Additionally, we have provided evidence for non-magnetic fractional quantization of conductance. Our experiments demonstrate that these states persist at elevated temperatures, are not spin-polarized, and their occurrence is preserved under one direction of lateral asymmetric bias while being suppressed in the opposite direction. This provides experimental support for the theoretical model presented in Ref. [41], which suggests that non-magnetic fractional conductance quantization can arise from strong electron-electron interactions and momentum-conserving backscattering between electrons in distinct subbands.

The data further suggests the potential formation of a zigzag incipient Wigner crystal, where backscattering between the two transverse channels could result in fraction formation and entanglement. Further investigation is required to elucidate the origin of these fractions and their associated subband configurations.

The unique properties of InAs combined with these fractional states suggest promising future applications in spintronic devices and quantum computing systems.

ACKNOWLEDGMENTS

The authors gratefully acknowledge financial support from the UK Science and Technology Facilities Council (Award No. ST/Y005074/1) and the EPSRC (Grant No. EP/R029075/1), which enabled the transport measurements, and the US Department of Energy (Award No. DESC0019274), which supported the growth and characterization efforts at UCSB. We also thank for the use of the shared facilities of the NSF Materials Research Science and Engineering Center (MRSEC) at the University of California Santa Barbara (Grant No. DMR 2308708), and the UCSB Nanofabrication Facility, an open access laboratory, and the SP Cleanroom at the University of Cambridge for access to their fabrication facilities.

- [1] D. A. Wharam, T. J. Thornton, R. Newbury, M. Pepper, H. Ahmed, J. E. F. Frost, D. G. Hasko, D. C. Peacock, D. A. Ritchie, and G. A. C. Jones, One-dimensional transport and the quantisation of the ballistic resistance, *J. Phys. C: Solid State Phys.* **21**, L209 (1988).
- [2] B. J. van Wees, H. van Houten, C. W. J. Beenakker, J. G. Williamson, L. P. Kouwenhoven, D. van der Marel, and C. T. Foxon, Quantized conductance of point contacts in a two-dimensional electron gas, *Phys. Rev. Lett.* **60**, 848 (1988).
- [3] N. K. Patel, J. T. Nicholls, L. Martin-Moreno, M. Pepper, J. E. F. Frost, D. A. Ritchie, and G. A. C. Jones, Evolution of half plateaus as a function of electric field in a ballistic quasi-one-dimensional constriction, *Phys. Rev. B* **44**, 13549 (1991).
- [4] T.-M. Chen, A. C. Graham, M. Pepper, I. Farrer, D. Anderson, G. A. C. Jones, and D. A. Ritchie, Direct observation of nonequilibrium spin population in quasi-one-dimensional nanostructures, *Nano Lett.* **10**, 2330 (2010).
- [5] T.-M. Chen, A. C. Graham, M. Pepper, I. Farrer, and D. A. Ritchie, Bias-controlled spin polarization in quantum wires, *Appl. Phys. Lett.* **93**, 032102 (2008).
- [6] K. J. Thomas, J. T. Nicholls, M. Y. Simmons, M. Pepper, D. R. Mace, and D. A. Ritchie, Possible spin polarization in a one-dimensional electron gas, *Phys. Rev. Lett.* **77**, 135 (1996).
- [7] K. J. Thomas, J. T. Nicholls, N. J. Appleyard, M. Y. Simmons, M. Pepper, D. R. Mace, W. R. Tribe, and D. A. Ritchie, Interaction effects in a one-dimensional constriction, *Phys. Rev. B* **58**, 4846 (1998).
- [8] K. J. Thomas, J. T. Nicholls, M. Pepper, W. R. Tribe, M. Y. Simmons, and D. A. Ritchie, Spin properties of low-density one-dimensional wires, *Phys. Rev. B* **61**, R13365(R) (2000).
- [9] A. Kristensen, H. Bruus, A. E. Hansen, J. B. Jensen, P. E. Lindelof, C. J. Marckmann, J. Nygård, C. B. Sørensen, F. Beuscher, A. Forchel, and M. Michel, Bias and temperature dependence of the 0.7 conductance anomaly in quantum point contacts, *Phys. Rev. B* **62**, 10950 (2000).
- [10] W. K. Hew, K. J. Thomas, M. Pepper, I. Farrer, D. Anderson, G. A. C. Jones, and D. A. Ritchie, Incipient formation of an electron lattice in a weakly confined quantum wire, *Phys. Rev. Lett.* **102**, 056804 (2009).
- [11] L. W. Smith, W. K. Hew, K. J. Thomas, M. Pepper, I. Farrer, D. Anderson, G. A. C. Jones, and D. A. Ritchie, Row coupling in an interacting quasi-one-dimensional quantum wire investigated using transport measurements, *Phys. Rev. B* **80**, 041306(R) (2009).
- [12] S. Kumar, K. J. Thomas, L. W. Smith, M. Pepper, G. L. Creeth, I. Farrer, D. Ritchie, G. Jones, and J. Griffiths, Many-body effects in a quasi-one-dimensional electron gas, *Phys. Rev. B* **90**, 201304(R) (2014).
- [13] S.-T. Lo, C.-H. Chen, J.-C. Fan, L. W. Smith, G. L. Creeth, C.-W. Chang, M. Pepper, J. P. Griffiths, I. Farrer, H. E. Beere, G. A. C. Jones, D. A. Ritchie, and T.-M. Chen, Controlled spatial separation of spins and coherent dynamics in spin-orbit-coupled nanostructures, *Nat. Commun.* **8**, 15997 (2017).
- [14] T.-M. Chen, M. Pepper, I. Farrer, G. A. C. Jones, and D. A. Ritchie, All-electrical injection and detection of a spin-polarized current using 1D conductors, *Phys. Rev. Lett.* **109**, 177202 (2012).
- [15] P. Chuang, S.-C. Ho, L. W. Smith, F. Sfigakis, M. Pepper, C.-H. Chen, J.-C. Fan, J. P. Griffiths, I. Farrer, H. E. Beere, G. A. C. Jones, D. A. Ritchie, and T.-M. Chen, All-electric all-semiconductor spin field-effect transistors, *Nature Nanotech.* **10**, 35 (2015).
- [16] B. Shojaei, P. J. J. O'Malley, J. Shabani, P. Roushan, B. D. Schultz, R. M. Lutchyn, C. Nayak, J. M. Martinis, and C. J. Palmström, Demonstration of gate control of spin splitting in a high-mobility InAs/AlSb two-dimensional electron gas, *Phys. Rev. B* **93**, 075302 (2016).
- [17] C. Thomas, A. T. Hatke, A. Tuaz, R. Kallaher, T. Wu, T. Wang, R. E. Diaz, G. C. Gardner, M. A. Capano, and M. J. Manfra, High-mobility InAs 2DEGs on GaSb substrates: A platform for mesoscopic quantum transport, *Phys. Rev. Mater.* **2**, 104602 (2018).
- [18] J. Shabani, A. P. McFadden, B. Shojaei, and C. J. Palmström, Gating of high-mobility InAs metamorphic heterostructures, *Appl. Phys. Lett.* **105**, 262105 (2014).
- [19] A. T. Hatke, T. Wang, C. Thomas, G. C. Gardner, and M. J. Manfra, Mobility in excess of 10^6 cm²/V s in InAs quantum wells grown on lattice mismatched InP substrates, *Appl. Phys. Lett.* **111**, 142106 (2017).
- [20] S. Mueller, C. Mittag, T. Tschirky, C. Charpentier, W. Wegscheider, K. Ensslin, and T. Ihn, Edge transport in InAs and InAs/GaSb quantum wells, *Phys. Rev. B* **96**, 075406 (2017).
- [21] C. P. Dempsey, J. T. Dong, I. Villar Rodriguez, Y. Gul, S. Chatterjee, M. Pendharkar, S. N. Holmes, M. Pepper, and C. Palmström, Effects of strain compensation on electron mobilities in InAs quantum wells grown on InP(001) (2024), arXiv:2406.19469.
- [22] A. Benali, P. Rajak, R. Ciancio, J. Plaisier, S. Heun, and G. Biasiol, Metamorphic InAs/InGaAs QWs with electron mobilities exceeding 7×10^5 cm²/Vs, *J. Cryst. Growth.* **593**, 126768 (2022).
- [23] J. Shabani, S. Das Sarma, and C. J. Palmström, An apparent metal-insulator transition in high-mobility two-dimensional InAs heterostructures, *Phys. Rev. B* **90**, 161303(R) (2014).
- [24] C. R. Pidgeon, D. L. Mitchell, and R. N. Brown, Interband magnetoabsorption in InAs and InSb, *Phys. Rev.* **154**, 737 (1967).
- [25] S. N. Holmes, P. J. Simmonds, H. E. Beere, F. Sfigakis, I. Farrer, D. A. Ritchie, and M. Pepper, Bychkov-Rashba dominated band structure in an In_{0.75}Ga_{0.25}As-In_{0.75}Al_{0.25}As device with spin-split carrier densities of $< 10^{11}$ cm⁻², *J. Phys.: Condens. Matter* **20**, 472207 (2008).
- [26] M. J. Snelling, G. P. Flinn, A. S. Plaut, R. T. Harley, A. C. Tropper, R. Eccleston, and C. C. Phillips, Magnetic g factor of electrons in GaAs/Al_xGa_{1-x}As quantum wells, *Phys. Rev. B* **44**, 11345 (1991).
- [27] A. Das, Y. Ronen, Y. Most, Y. Oreg, M. Heiblum, and H. Shtrikman, Zero-bias peaks and splitting in an Al-InAs nanowire topological superconductor as a signature of Majorana fermions, *Nature Phys.* **8**, 887 (2012).
- [28] R. M. Lutchyn, J. D. Sau, and S. Das Sarma, Majorana fermions and a topological phase transition in

- semiconductor-superconductor heterostructures, Phys. Rev. Lett. **105**, 077001 (2010).
- [29] Y. Oreg, G. Refael, and F. von Oppen, Helical liquids and Majorana bound states in quantum wires, Phys. Rev. Lett. **105**, 177002 (2010).
- [30] Microsoft Azure Quantum., Interferometric single-shot parity measurement in InAs–Al hybrid devices, Nature **638**, 651–655 (2025).
- [31] S. Sarma, M. Freedman, and C. Nayak, Majorana zero modes and topological quantum computation, npj Quantum Inf **1**, 15001 (2015).
- [32] S. Matsuo, H. Kamata, S. Baba, R. S. Deacon, J. Shabani, C. J. Palmström, and S. Tarucha, Magnetic field inducing Zeeman splitting and anomalous conductance reduction of half-integer quantized plateaus in InAs quantum wires, Phys. Rev. B **96**, 201404(R) (2017).
- [33] C. Mittag, M. Karalic, Z. Lei, C. Thomas, A. Tuaz, A. T. Hatke, G. C. Gardner, M. J. Manfra, T. Ihn, and K. Ensslin, Gate-defined quantum point contact in an InAs two-dimensional electron gas, Phys. Rev. B **100**, 075422 (2019).
- [34] J. S. Lee, B. Shojaei, M. Pendharkar, A. P. McFadden, Y. Kim, H. J. Suominen, M. Kjaergaard, F. Nichele, H. Zhang, C. M. Marcus, and C. J. Palmström, Transport studies of epi-Al/InAs two-dimensional electron gas systems for required building-blocks in topological superconductor networks, Nano Lett. **19**, 3083 (2019).
- [35] C. L. Hsueh, P. Sriram, T. Wang, C. Thomas, G. Gardner, M. A. Kastner, M. J. Manfra, and D. Goldhaber-Gordon, Clean quantum point contacts in an InAs quantum well grown on a lattice-mismatched InP substrate, Phys. Rev. B **105**, 195303 (2022).
- [36] Y. Gul, S. N. Holmes, M. Myronov, S. Kumar, and M. Pepper, Self-organised fractional quantisation in a hole quantum wire, J. Phys.: Condens. Matter **30**, 09LT01 (2018).
- [37] L. Liu, Y. Gul, S. N. Holmes, C. Chen, I. Farrer, D. A. Ritchie, and M. Pepper, Possible zero-magnetic field fractional quantization in In_{0.75}Ga_{0.25}As heterostructures, Appl. Phys. Lett. **123**, 183502 (2023).
- [38] S. Kumar, M. Pepper, S. N. Holmes, H. Montagu, Y. Gul, D. A. Ritchie, and I. Farrer, Zero-magnetic field fractional quantum states, Phys. Rev. Lett. **122**, 086803 (2019).
- [39] C. Ford, *CryoMeas — A Data-Acquisition Program for LabView*, The University of Cambridge (2023).
- [40] Y. Gul, G. L. Creeth, D. English, S. N. Holmes, K. J. Thomas, I. Farrer, D. J. Ellis, D. A. Ritchie, and M. Pepper, Conductance quantisation in patterned gate In_{0.75}Ga_{0.25}As structures up to $6 \times (2e^2/h)$, J. Phys.: Condens. Matter **31**, 104002 (2019).
- [41] G. Shavit and Y. Oreg, Fractional conductance in strongly interacting 1D systems, Phys. Rev. Lett. **123**, 036803 (2019).
- [42] L. Saminadayar, D. Glattli, Y. Jin, and B. Etienne, Observation of the $e/3$ fractionally charged Laughlin quasiparticle, Phys. Rev. Lett. **79**, 2526 (1997).
- [43] A. Bid, N. Ofek, M. Heiblum, V. Umansky, and D. Mahalu, Shot noise and charge at the $2/3$ composite fractional quantum Hall state, Phys. Rev. Lett. **103**, 236802 (2009).
- [44] R. de Picciotto, M. Reznikov, M. Heiblum, V. Umansky, G. Bunin, and D. Mahalu, Direct observation of a fractional charge, Nature **389**, 162–164 (1997).
- [45] M. Reznikov, R. de Picciotto, T. Griffiths, M. Heiblum, and V. Umansky, Observation of quasiparticles with one-fifth of an electron’s charge, Nature **399**, 238–241 (1999).
- [46] M. Dolev, M. Heiblum, V. Umansky, A. Stern, and D. Mahalu, Observation of a quarter of an electron charge at the $\nu = 5/2$ quantum Hall state, Nature **452**, 829–834 (2008).